Journal of Theoretical and Applied Information Technology
31st March 2023. Vol.101. No 6

ISSN: 1992-8645 www.jatit.org E-ISSN: 1817-3195

OCHOA-RNN: OPPOSITIONAL BASED CHIMP OPTIMIZATION ALGORITHM (OCHOA) AND RECURRENT NEURAL NETWORK (RNN) HYBRID CLASSIFIER MODEL FOR LUNG CANCER DIAGNOSIS

[1]JENITA SUBASH, [2]DR.KALAIVANI.S*

[1]Research Scholar, School of Electronics Engineering (SENSE), Vellore Institute of Technology,

Vellore, Tamil Nadu, India

Jenita.subash2014@vit.ac.in

[2]Associate Professor, *Corresponding Author, School of Electronics Engineering (SENSE), Vellore Institute of Technology,

Vellore, Tamil Nadu , India

ABSTRACT

One of the prominent reasons of cancer-related mortality in this world is "Lung Cancer". Therefore, precautions such as detection, prediction and diagnosis of lung cancer have become essential to be expedited and simplified the consequent clinical board. An Artificial Intelligence technique has been proposed as promising tool for classifying normal, benign and malignant nodules. The research aim is to retrospectively validate Lung Cancer Prediction through Oppositional based Chimp Optimization Algorithm (OChOA) in associates with (LSTM)Recurrent Neural Network. The investigation anticipates using various optimization techniques namely ChOA, Social Spider Optimization (SSO), Particle Swarm Optimization (PSO), Genetic Algorithm (GA) for identifying optimal weights for RNN. The result shows that involving optimization for identifying weights forLSTM- RNN unveils 97.13% from the proposed OChOA-RNN.

Keyword: *Lung cancer, Recurrent Neural Network, Oppositional based Chimp Optimization Algorithm, Long Short-Term Memory, CT images, bengin and malignant.*

1. INTRODUCTION

Cancer is primary diseases to lead a large number of fatalities worldwide. Lung cancer is the most chronic form of cancer than other major types of cancers [1]. Also, lung cancer is second most prevailing cancer in men and women [2]. Additionally, lung cancer-related diseases have been most common causes of deaths worldwide [3]. According to a global survey of WHO, 1.8 billion people have been suffering from lung cancer [4], nearly 1.6 million people are dying where breast cancer becomes the second reason for death. Based on USA survey, even after affected by lung cancer, nearly 5 years, 17.4% of people manage survival. Additionally, the report presented by North American Association of Central Cancer Registries [5] in 2018 in USA , 13% of women (112,350) and 14% of men (121,680) are suffering from lung cancer where 154,040 people was died because of high risk factors of lung cancer. Lung carcinoma is another term for lung cancer [6] that affects the person because of the abnormal tissues growth in lung. Lung cancer is a multi-step and multi-factorial disease, has a various histological subtypes, which is known as most worldwide fatal cancer. Etiology of lung cancer is yet unsolved. Air pollution and Smoking can be two prominent risk factors. Other risk factors namely occupational exposure (for example asbestos) which is also crucial cause for lung cancer development [7]. In addition, lung cancer is heterogeneous disease, environmental exposures and constitutional genetic or epigenetic susceptibilities are major impacts to disease development and progression [8]. Generally, lung cancer can be divided into two various types with various methodologies of treatment: non-small cell lung carcinoma and small cell lung carcinoma are two lung cancer categories [9]. Since cancer symptoms normally appear only during advanced stages which are difficult to detect and leads to high mortality rate than other cancer types. Hence, it is

necessary to predict lung cancer as early as for diagnosing purpose and this can result in better chances for successful treatment [10]. Thereby, early lung cancer detection enhances cure chances. Consequently, it leads to higher survival rates [11]. For example, NLST (National Lung Screening Trial) showed scanning with LDCT (low-dose computed tomography) reduced about 20% for rate of mortality in population with high-risk [12]. However, early lung cancer diagnosis has numerous challenges. In particular, pulmonary cancer detection during the early stages is difficult mainly due to the presence of lesion growth about dime-size in lung known as nodule. Initial step towards lung cancer cure will be the lung nodules detection during their early stage and it can be treated before the malignant stage [13]. Hence, they need for sensitive and reliable tools during the preclinical diagnosis of lung cancer [14]. Radiological imaging methods namely CT (computed tomography) and CXR (chest digital X-ray) are standard tools for screening utilized during detecting as well as diagnosing chest respiratory diseases early during clinical course, including lung cancer [15]. Among these, X-ray is the traditional technique for the lung cancer detection. It is the process of mass screening through X-ray films. But, small nodules of lung cancer cannot be easily detected by X-ray in an early stage due to the shadow of organ and the overlapping of bone [13]. Alternatively, the CT chest imaging modality can be highly preferable in early lung cancer detection and diagnosis [16]. But, computer-aided diagnosis (CADx) scheme has been suggested and established to be "second reader" help radiologists in decision making due to its difficult, tedious, and time-consuming process for diagnosing pulmonary nodules based on CT images [17]. Moreover, pulmonary (lung) nodule detection automation with effective and efficient tools of CAD facilitates radiologists in a fast diagnosis which enhances diagnostic confidence. Between certain techniques, dealing with variations of morphological in nodules that are seen in CT images is key challenge in CAD systems for lung cancer [18]. That means, CAD system has limitations like fails for diagnosing subtle regions and high false positives in lung cancer [19]. Therefore, to overcome this, a lot of CAD systems based on artificial intelligence method help radiologists detecting and classifying lung nodule for early diagnosis of lung cancer [20]. For example, Probabilistic Neural Network (PNN) [21], Improved Deep Neural Network And Ensemble Classifier (IDNN) [22], SVM (Support Vector Machine) Classifier, MLP (Multi-Layer Perceptron) classifier, KNN (K-Nearest Neighbors) Classifier, DT (Decision Tree) Classifier, SGD (Stochastic Gradient Descent) Classifier, RF (Random Forest) Classifier, and MNB (Multinomial Naive Bayes) Classifier [23]. However, the performance and accuracy of these methods have not been enough. Since medical treatment itself is a very professional and accurate field. Hence, to accurately detect lung cancer, Long Short-Term Memory with Chimp Optimization Algorithm-based technique is proposed in this paper.

2. LITERATURE REVIEW

Accurate LCD (Lung Cancer Disease) diagnosis is the crucial process for treating timely the patients suffering from lung cancer. ALzubi et al. (2019) [24] had proposed and analyzed WONN-MLB (Weight Optimized Neural Network with Maximum Likelihood Boosting) ensemble on LCD within big data. Feature selection and ensemble classification were categorized as two stages of proposed technique. During primary stage, essential attributes were chosen with pre-processing model of integrated Newton–Raphsons MLMR (Maximum Likelihood and Minimum Redundancy) minimize time of classification. During secondary stage, technique of Boosted Weighted Optimized Neural Network Ensemble Classification was classified patient with selected attributes and enhanced accuracy of cancer disease diagnosis that reduce false positive rate. While comparing with traditional methods, experimental results demonstrated proposed technique to attain reduced delay, better false positive rate and accuracy of prediction.

Shakeel et al. (2020) [25] had introduced the effective as well as optimized methods of neural computing and soft computing for reducing issues as well as difficulties in set of feature. At first, ELVIRA Biomedical Data Set Repository, biomedical data of lung can be gathered. Presence of noise within data can be removed using process of bin smoothing normalization. Wolf heuristic features and Minimum repetition often chose for reducing features' complexity as well as dimensionality. The data was analysed chosen features of lung utilizing Discrete AdaBoost optimized ensemble learning generalized neural networks that analysed pulmonary biomedical data as well as categorized features of normal and abnormal with tremendous effectiveness. System efficiency can be examined through MATLAB experimental setup regarding precision, G-mean, recall F-measure, rate of prediction and error rate.

To detect lung cancer, Shakeel et al. (2019) [26] proposed enhanced profuse clustering and deep learning instantaneously trained neural networks. Study dealt with improvement of lung image quality and lung cancer diagnosis through minimizing misclassification. CT images of lung were gathered from dataset of CIA (Cancer imaging Archive), presence of noise within images were removed using weighted mean histogram equalization technique that often eliminates noise from image, also improves image quality through IPCT (improved profuse clustering technique) to segment affected region. Affected region yielded different spectral features. To predict lung cancer, it can be evaluated using deep learning instantaneously trained neural network. By MATLAB based simulation results, system was tested through system efficiency. With minimum error of classification of 0.038, System ensured 98.42% accuracy.

Varadharajan et al. (2018) [27] had proposed investigation for testing expectation of lung tumour by classification algorithms such as decision tree and back propogation neural network. Initially, using classification algorithms, examples 20 tumour as well as non-disease patients' data get gathered with 30 qualities, pre-prepared and dissected whereas the same methodology can be actualized on 50 happenings (10 non growth patients as well as 50 Cancer patients). Using WEKA Tool, principle point of study gave prior notice to the clients which quantified execution investigation of classification methods. Test demonstrates aforementioned calculation with promising results for similar cause having exactness of general forecast of 94 and 95.4%, respectively. Alternatively, identifying lungs tumour through Decision tree and BPNN calculation would provide authentic result in contrast with remaining calculation. Proposed framework would enhance execution of classification as well as prediction.

Early lung cancer detection enhances survival chance of patient. CT (Computed Tomography) scan helps to discover tumor position and identify cancer level in the body. Lakshmanaprabu et al. (2019) [28] had presented an innovative automated diagnosis classification technique in lungs' CT scans. In this study, CT lung images analysed using ODNN (Optimal Deep Neural Network) and LDA (Linear Discriminate Analysis). Deep features extracted from CT images of lung whereas feature dimensionality was decreased through LDR for classifying nodules of lung to be malignant or benign. ODNN was used for CT images which optimized through MGSA (Modified Gravitational Search Algorithm) to discover classification of lung cancer. Comparative outcomes indicate proposed classifier to give specificity 94.2%, accuracy 94.56% and sensitivity 96.2%.

Schwyzer et al. (2018) [29] had studied the assistance of machine learning for lung cancer detection while FDG-PET imaging during ultralow dose PET scans setting. Without pulmonary malignancies, authors had evaluated ANN (artificial neural network) performance discriminating patients with lung cancer (n=50) from controls (n=50). 0 For detection of lung cancer, the area under deep learning algorithm curve can be 0.989, 0.983 and 0.970 to images of standard dose (PET100%), which decreased the dose about reconstruction of PET10%, as well as PET3.3%, separately. In standard dose as well as ultralow dose PET3.3% separately, ANN attained sensitivity between 95.9% and 91.5% whereas specificity between 98.1% and 94.2%. The results suggested machine learning methods to be helpful in detection of automated lung cancer even in doses with low effective radiation about 0.11 mSv.

3. PROPOSED METHODOLOGY

The research initiate with extracting the object from the actual image using ROI followed by the denoising process. The denoising process consists of three phases namely, image decomposition using Optimal Discrete Wavelet Transform (ODWT), second stage noise removal using Block Matching, and 3D filtering (BM3D) filter and third stage noise removal using the adaptive bilateral filter (ABF). The subsequent feature extraction process carried out with GLCM (Gray-Level Co-Occurrence Matrix) with different orientation (0, 45, 90, and 135) and DWT features. Eventually, the research considers LSTM (Long Short-Term Memory) networks are RNN (Recurrent Neural Network) type capable of learning order dependence in problems of sequence prediction. These layers, built into a network, function as some sort of memory that allows the network to infer from not only the present, but also past events. The research utilizes the LSTM to diagnose the lung condition like Normal, Benign and Malignant. It is evident from the literature that RNN based LSTM having proficient performance over other comparative techniques. Even though RNN based LSTM shows tremendous performance, there are some drawbacks in predicting performance.

To enhance the performance of the existing method, this research involves hyper parameter optimization for a learning algorithm to resolve the existing complexities. A hyper parameter is a parameter whose value control learning process. This research involves various existing optimization techniques like GA (Genetic Algorithm), PSO (Particle Swarm Optimization), SSO (Social Spider Optimization) and ChOA (Chimp Optimization Algorithm), which can be inspired through chimps' individual intelligence and sexual motivation during group hunting that is varied from remaining social predators. During solving high-dimensional problems, ChOA can be formulated to further reduce two difficulties like slow convergence speed and trapping within local optimum. Additionally, oppositional based strategy involves with ChOA is designed for enhance the performance of the conventional technique. The block diagram of OChOA-RNN: Oppositional based Chimp Optimization Algorithm (OChOA) in association with Recurrent Neural Network (RNN) Hybrid classifier model is given in Fig.1 and Fig.2.

Figure.1 Block diagram of OChOA-RNN: Oppositional based Chimp Optimization Algorithm (OChOA) in association with Recurrent Neural Network (RNN) Hybrid

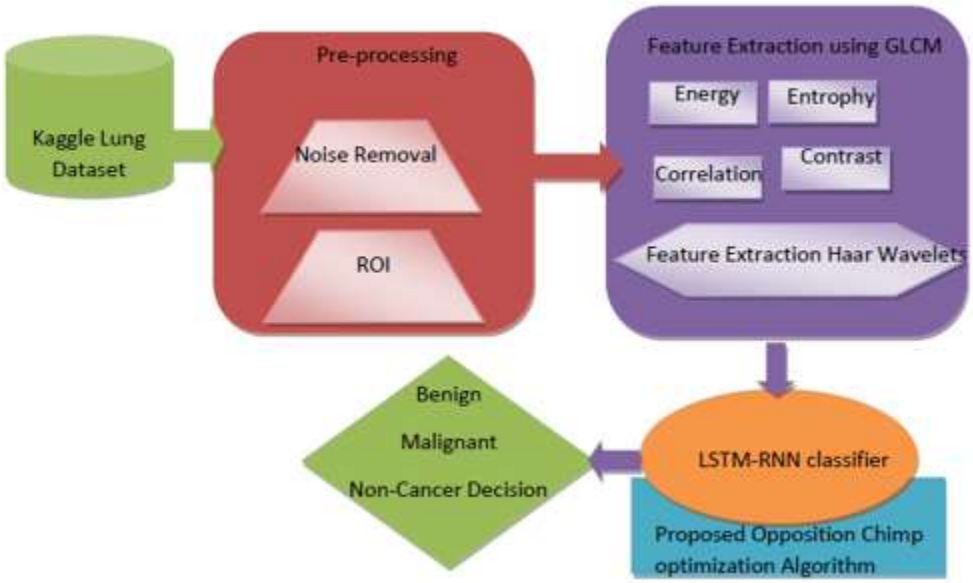

Figure 2. OChOA-RNN: Oppositional based Chimp Optimization Algorithm (OChOA) in association with Recurrent Neural Network (RNN) Hybrid classifier model

Datasets used:

The Iraq-Oncology Teaching Hospital/National Center for Cancer Diseases (IQ-OTH/NCCD) lung cancer dataset was collected in the above-mentioned specialist hospitals over a period of three months in fall 2019. It includes CT scans of patients diagnosed with lung cancer in different stages, as well as healthy subjects. IQ-OTH/NCCD slide were annotated by oncologists and radiologists in the two centers .The dataset contains a total of 1190 images representing CT scans slices of 110 cases. These cases are grouped into three classes: normal, benign, and malignant. of these, 40 cases are diagnosed as malignant; 15 cases diagnosed with benign; and 55 cases

classified as normal cases.Fig.3 shows sample CT images from IQ-OTH/NCCD dataset

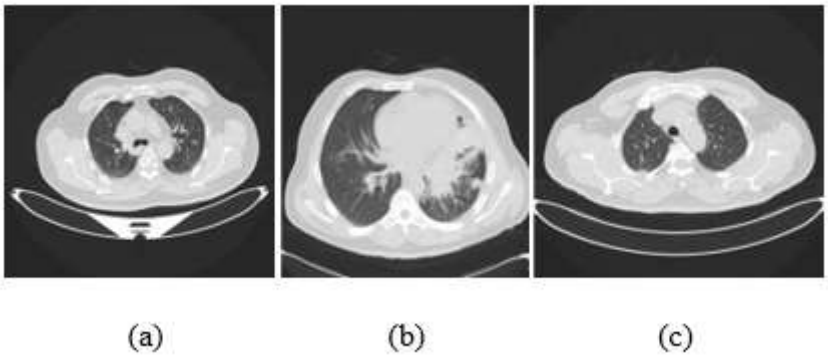

Fig .3 Sample CT Images From IQ-OTH/NCCD Dataset (A) Benign (B) Malignant (C) Normal Case

4. GLCM

Probabilities of co-occurrence give second order technique to generate features of texture. Haralick followed brief presentation of GLCM technique with more complete explanation [30,31]. Two parameters: (i) interpixel distance (d), (ii) interpixel orientation (φ), Matrix has probabilities of conditional joint for every pair wise combinations of gray levels. Probability measure is formulated based on Barber [32]:

$$p_r(x) = \{C_{ij} | (d, \theta)\} \quad (1)$$

here C_{ij} (GLCM) can be formulated:

$$c_{ij} = \frac{P_{ij}}{\sum_{i,j=1}^{c} P_{ij}} \quad (2)$$

Number of gray levels occurrences g_i and g_j denoted by P_{ij} whereas total gray levels meant by G. In window given particular (d, φ), total gray level pairs is denoted by sum in denominator. Varied GLCM could be needed for each (d, φ). Distances of Pixel separation (d) can be generally less than degrees of 10. 0, 45, 90 and 135. 180 degrees of orientation will be redundant to 0 degrees, 225 degrees of orientation will be redundant to 45 degrees, and so on are typically, only four orientations that can be utilized in computation simplicity/

GLCM texture statistics defined	
MAX (Maximum probability)	$\mathbf{Max\{C_{ij} V(I,j)\}}$
ENG (Energy)	$\sum_{i,j=1}^{c} c_{i,j}^2$
ENT (Entropy)	$\sum_{i,j=1}^{c} c_{ij} \log c_{ij}$
DIS (Dissimilarity)	$\sum_{i,j=1}^{c} \lvert i-j \rvert$
CON (Contrast)	$-\sum_{i,j=1}^{c} c_{ij}(i-j)^2$
HOM (Homogeneity)	$\sum_{i,j=1}^{c} \frac{1}{1=\lvert i-j \rvert}$
IDM (Inverse Difference Moment)	$\sum_{i,j=1}^{c} \frac{1}{1+(i-j)^2/c^2}$
COR (Correlation)	$\sum_{i,j=1}^{c} \frac{(i-\mu)(j-\mu)}{\sigma_i \sigma_j}$

While invariance to spatial rotations is desired, average of four orientations is utilized. Every GLCM determines different statistical information; nevertheless, statistics are gray level shift invariant as significant for classification that is not tone function. There are eight different shift invariant statistics can be provided.

4.1 GLCM approach

Distance between pixel pair d and its angular relationship φ are two parameters used in GLCM based defect detection calculated. In four directions (0◦ , 45◦ , 90◦ and 135◦), former researches usually quantified φ. In small window that scans entire image, GLCM can be computed. All images of non-defective as well as defective are needed conversion of gray scale, before calculating GLCM. Resolution of test images obtained from camera is about 512 × 512 pixels. Resulting GLCM can be calculated over numerous displacements where distances get differed from 1 pixel to range of full dynamic whereas angles will be 0° (that is, horizontal offset in GLCM in MATLAB). In [33],

for faster processing, region of real time of interest cropping has been explained. GLCM can be normalized whereas GLCM shows probabilities other than counts before calculation of texture. Total counted pixel pairs divides involved normalization.

Offset of horizontal is taken into account, which makes algorithm to run quickly. COR, ENG, HOM and CON are four characteristics of GLCM that can be taken here. In scheme of defect detection, for smaller size of window, four features presented good outcomes. Four EFM (elemental feature matrices) are derived for each d value. This technique is quicker than previous algorithm one since this only examines horizontal offsets having small size of window about 10 × 10. Then, with the assistance of four features using various d values, compute different non-defective template image's statistical data. Simultaneously for obtained test images and statistical information can be distinguished. When these can be similar, there will be no defect. Otherwise, sample can be defected. Table 1 sows sample features extracted using GLCM.

Table . 1 Sample Features Extracted Using GLCM

	Contrast	Correlation	Energy	Homogeneity	Maximum probability	IDM	Dissimilarity	Entropy
Bengin case (78)	0.069471624	0.993669	0.433485	0.980519	0.610594	0.998977	0.045889	1.243425
Bengin case (79)	0.071015778	0.993477	0.431683	0.980511	0.60939	0.998956	0.046202	1.249377
Bengin case (8)	0.076221563	0.992964	0.447259	0.978759	0.626644	0.998878	0.050124	1.23893
Malignant case (532)	0.056273697	0.995138	0.316768	0.980259	0.437641	0.999158	0.043355	1.527815
Malignant case (533)	0.056055834	0.995118	0.31369	0.980312	0.434511	0.999161	0.043221	1.53502
Malignant case (534)	0.058287977	0.994869	0.309916	0.979732	0.429951	0.999129	0.044597	1.545956
Normal case (406)	0.066119588	0.994389	0.413908	0.978994	0.584221	0.999017	0.04759	1.27522
Normal case (407)	0.065542441	0.994398	0.413958	0.978933	0.583835	0.999024	0.047571	1.278236
Normal case (408)	0.065179336	0.994405	0.412211	0.978626	0.583033	0.999027	0.04801	1.285919

4.2 Haar Wavelet

Haar wavelet family for x ∈ [0, 1] can be explained:

$$h_i(x)=\begin{cases}1 & for\, x\in[\xi_1,\xi_2),\\ -1 & for\, x\in[\xi_2,\xi_3),\\ 0 & elsewhere\end{cases} \quad (3)$$

Here,

$$\xi_1=\frac{k}{m},\ \xi_2=\frac{k+0.5}{m},\ \xi_3=\frac{k+1}{m}. \quad (4)$$

Here, integer $m=2^j$, j = 0, 1,…. j indicates level of wavelet; translation parameter is meant by k = 0, 1, ….m – 1. Maximal resolution level can be denoted by j. In Equation (3), in case of minimal values m = 1, k=0 there is, i = 2; Index I has computed from i = m+ k + 1. $i = 2M = 2^{j+1}$ is maximal i value. This can be reasonable to infer about value i = 1 corresponds with function of scaling

$$h_i(x)=\begin{cases}1 & for\ x\in[-1,1),\\ 0 & elsewhere\end{cases} \quad (5)$$

In below, wavelets' analysis integrals

$$p_i(x)=\int_0^x h_i(x)\,dx,$$
$$q_i(x)=\int_0^x p_i(x)dx \quad (6)$$

needed to be calculated. It will be completed using (3):

$$p_i(x)=\begin{cases}x-\xi_1 & for\, x\in[\xi_1,\xi_2),\\ \xi_3-x & for\, x\in[\xi_2,\xi_3),\\ 0 & elsewhere,\end{cases} \quad (7)$$

$$q_i(x)=\begin{cases}0 & for\ x\in[0,\xi_1),\\ 0.5(x-\xi_1)^2 & for\ x\in[\xi_1,\xi_2),\\ \frac{1}{4m^2}-\frac{1}{2}(\xi_3-x)^2 & for\ x\in[\xi_2,\xi_3),\\ \frac{1}{4m^2} & for\ x\in[\xi_3,1),\end{cases} \quad (8)$$

In this study, wavelet-collocation technique has been used. The collocation points can be formulated:

$$x_l=(l-0.5)/(2M),\quad l=1,2.....,2M. \quad (9)$$

$2M$ X $2M$ matrices H, P, Q with elements $H(i,l)=hi(x_l)$, $p(I,l)=p_i(x_l)$, $Q(i,l)=qi(x_l)$ has conveniently introduced. Table 2 sows sample features extracted using Haar Wavelets.

Table . 2 Sample Features Extracted Using Haar Wavelets

	CA-mean	CH-mean	CV-mean	CD-mean	CA-SD	CH-SD	CV-SD	CD-SD
Bengin case (78)	0.777871	-0.00033	-4.53E-05	-2.46E-05	0.163812	0.011997	0.009883	0.003475
Bengin case (79)	0.775784	-0.00034	-4.79E-05	-2.24E-05	0.16349	0.012236	0.010542	0.003228
Bengin case (8)	0.758852	-0.00031	-3.38E-05	-1.43E-05	0.187781	0.013319	0.011811	0.003475
Malignant case (532)	0.964439	-0.00029	-0.00026	-5.78E-06	0.083865	0.004327	0.010226	0.002352
Malignant case (533)	0.9591	-0.00029	-0.00024	4.62E-07	0.086778	0.004153	0.01035	0.002324
Malignant case (534)	0.954893	-0.00029	-0.00022	-2.81E-06	0.088663	0.003982	0.010277	0.002306
Normal case (406)	0.834705	-0.00053	-4.48E-05	-1.98E-05	0.11204	0.006264	0.009609	0.002788
Normal case (407)	0.833433	-0.00055	-3.15E-05	-1.66E-05	0.112817	0.006309	0.009176	0.002724
Normal case (408)	0.831292	-0.00053	-2.34E-05	-1.98E-05	0.113753	0.006327	0.009242	0.002705

4.3 Proposed OChOA -Recurrent Neural Network

The training procedure of LSTM- RNN classifier is performed using proposed OChOA algorithm. The weight of the LSTM- RNN classifier classifier is trained using the proposed OChOA for obtaining optimal solution.

RNN can be defined as ANN with arbitrary connections between neurons (Fausett, 1994), fully connected among adjacent layers. The network nodes get input from current data point $x(t)$ and hidden state values of hidden layer in previous state $h(t-1)$. Hence, inputs at time t influences network outputs to receive in future through recurrent connections. Using iterating equations (10) and (11) over $t = 1, \ldots, T$. typical RNN with input vector $v=(v_1,\ldots v_T)$ computes hidden vector $h=h(h_1,\ldots h_T)$ whereas output vector $y=(y_1,\ldots y_T)$

$$h(t) = Q(W_{(hx)}\, x^{(t)} + W_{(hh)} h^{(t-1)} + b_h) \quad (10)$$

$$y^{(t)} = \sigma(W_{(yh)} h^{(t)} + b_y) \quad (11)$$

Here: b_y and b_h are vectors of biases,

Weights matrices of recurrent connections, layers of input-hidden and hidden-output are indicated as $W_{(yh)}$, $W_{(h,x)}$ and $W_{(hh)}$ respectively. Q is an activation function.

Backpropagation over time algorithm can use to train Standard neural networks across multiple time steps.

4.3.1 Long Term Short Term Memory Networks

From 1980s, LSTM networks have their origins within RNN and are RNN (recurrent neural network) architecture. Hochreiter and Schmidhuber were designed for addressing typical RNNs' vanishing and exploding gradient problems [34-36]. Architecture permits for accumulating data in operation which utilized feedback to remember previous network call states. In comparison to standard RNNs, LSTM (Long Short-Term Memory) model expressed exceptional capacity to learn long-range dependencies in practical applications. Hence, LSTM model is preferred by majority of modern applications. Generally, LSTM is made up of some memory blocks. Memory cells and gates make up Memory block. Memory cells are capable of remembering network's temporal state through self-connections whereas control information of gates flows. Every block of memory has gate of input to control input activations flow into cell of memory, gate of output to control cell activations output flow into the remaining network and forget gate. Figure 4 shows architecture of LSTM cell.

Moreover, there are three gates and two nodes in LSTM cell that act as a network interface for information propagation. Every LSTM cell has three various gates:

- *input gate* t_c^T which regulates activations of input into element of memory,
- *output gate* O_c^t regulates cell activations outflow into remaining of network,
- *forget gatef* f_c^t scales cell's internal state before summing to input using cell's self-recurrent connection. It allows for gradual forgetting within memory of cell.

In addition, cell of LSTM consists of internal state node s_c^t as well as an input node g_c^t

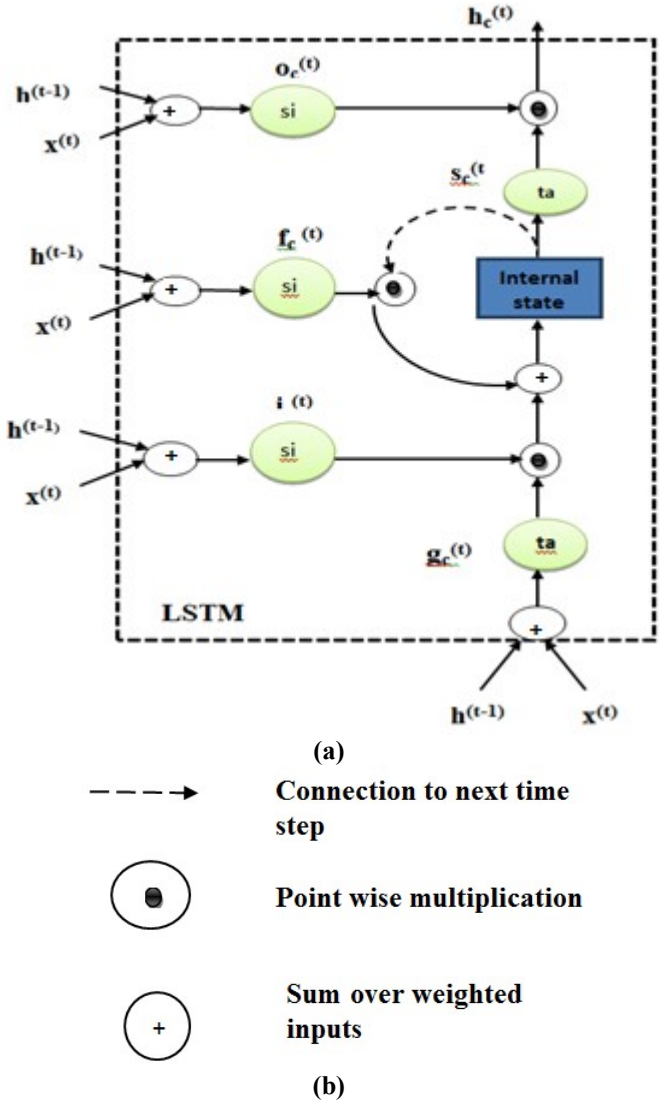

Figure 4: An Architecture Of LSTM Cell

Output of cells set of LSTM can be computed using vector equations below:

$$g^{(t)} = \phi(W_{gx} x^{(t)} + W_{gh} h^{(t-1)} + b_g) \quad (12)$$

$$i^{(t)} = \sigma(W_{ix} x^{(t)} + W_{ih} h^{(t-1)} + b_i) \quad (13)$$

$$f^{(t)} = \sigma(W_{fx} x^{(t)} + W_{fh} h^{(t-1)} + b_f) \quad (14)$$

$$O^{(t)} = \sigma(W_{ox} x^{(t)} + W_{oh} h^{(t-1)} + b_o) \quad (15)$$

where $x^{(t)}$ means input vector to unit of LSTM, $f^{(t)}$ means activation vector of forget gate, $f^{(t)}$ means activation vector of input gate, $o^{(t)}$ means activation vector of output gate.

During examining equations (23) – (26), this gets noticed the example of current and former step can be utilized in value of hidden layer's output vector h and in internal state vector s. This could be essential for taking down that equations have vector notation. They are addressed to entire LSTM cell set. The network of LSTM understands when to allow their cells' internal states activation and when to allow their outputs activation. With their learning capability, all the gates in this gating mechanism can be taken as distinct components of LSTM cell. This implies that cells must adapt in process of

training to maintain proper flow of information across the network as separate units. Hence, internal state of cell can be unaffected while the gates are closed. To accomplish this, function of hard sigmoid σ was utilized and output 0 and 1 to be provided in equation (16). Consequently, the gates are either fully closed or fully opened [37].

$$\sigma(x)=\begin{cases}0 \; if \; x\le t_1,\\ ax+b \; if \; x\in(t_l,t_h),\\ 1 if \; x\ge t_h \; .\end{cases} \quad (16)$$

Constant error carousel allows gradient for propagating back by several steps regarding backward pass. Also, in order to reduce the error value of RNN output, an enhanced BSO algorithm is employed for selecting the weight parameters of RNN and discussed in detail in next section.

4.4 Chimp optimization algorithm

Khishe, M., and Mohammad Reza Mosavi (2020) had proposed a novel metaheuristic algorithm known as ChOA (Chimp Optimization Algorithm) which was influenced through chimps' sexual motivation and individual intelligence during group hunting. It can be varied from remaining social predators.

4.4.1 Inspiration

ChOA is one of the metaheuristic algorithms that have been influenced through chimps' individual intelligence and sexual motivation during group hunting, which can be varied from existing social predators.

Chimps (often known as Chimpanzees) are only two African great ape species. They are closest living relatives of human. Due to derived from a single species of ancestor (Hominoid) existed before seven or eight million years, DNA of human as well as Chimpanzees are so similar. Colony of chimp is society of fission-fusion. Colony's combination or size fluctuates while time passes and individuals migrate across environment about the surroundings in this type of civilization. During this method, every chimps group independently tries to find search space using their technique. Chimpanzees cannot to be same regarding intelligence as well as ability in every group, but they are all doing their duties as a colony member. During particular situation**,** each individual's ability is helpful

In colony of chimp, driver, barrier, chaser, and attackers with various capabilities are four types of chimps. But such diversities require for a successful hunt. The prey is pursued by the drivers without getting too close to them. Barriers stay in a tree to create a dam that prevents from prey progression. To get near with them, chasers move rapidly behind the prey. At last, attackers prognosticate prey's breakout route to infliction them (prey) down into lower canopy or back towards chasers. Attackers may require lots of cognitive endeavour to prognosticate prey's subsequent movements. After a successful hunt, they are remunerated with larger meat piece. Age, smartness, and physical ability positively relate the prominent role (attacking). Additionally, chimps alter duties in similar hunt or keep their similar duty in whole process.

Additionally, these social incentives have only proposed for chimps. Therefore, this represents significant variation among existing social predators and chimps regarding cognitive ability. During last stage of hunting process, such social incentive (sexual motivation) makes chimpanzees perform chaotically and entire chimps will be abandoning the assigned tasks and frantically try to hunt down prey. On whole, chimps' hunting process can be categorized into two primary phases: driving, blocking, and chasing the prey are comprised by Exploration whereas attacking the prey is comprised by Exploitation. After that, such ChOA concepts can be mathematically designed below.

4.4.2 Mathematical model and algorithm

Here, driving, blocking, chasing, and attacking have been discussed mathematical models of an independent group. Corresponding algorithm of ChOA has been specified.

Driving and chasing the prey

Aforementioned, prey can be hunted in phases of exploration and exploitation. Equation. (17) and (18) can be proposed to mathematically model driving as well as chasing,

$$d=\left|c.x_{prey}(t)-m.x_{chimp}(t)\right| \quad (17)$$

$$x_{chimp}(t+1)=x_{prey}(t)-a.d \quad (18)$$

Here, number of the current iteration indicated by t, coefficient vectors indicated as a, m, and c, vector of prey position meant by X_{prey} whereas X_{chimp} denotes chimp's position vector. a, m, and c vectors have been computed in equations (3) – (5), separately.

$$a=2.f.r_1-f \quad (19)$$

$$c=2.r_2 \quad (20)$$

$$m=chaotic\_value \quad (21)$$

Here, **f** can be non-linearly decreased from 2.5 to 0 using process of iteration (in phase of

exploitation as well as exploration). Here $\mathbf{r_1}$ as well as $\mathbf{r_2}$ represent random vectors within range [0,1]. At last, **m** is chaotic vector computed on basis of different chaotic map where the vector means chimps' sexual motivation effect during process of hunting.

This concept is generalized for n-dimensional search space. Like said in former section, chimps can attack prey with chaotic strategy. Such technique can be mathematically formulated below.

Attacking method (exploitation phase)

Two methods have been formulated to mathematically model chimps' attacking behaviour: They have ability to explore location of prey (using driving, blocking and chasing) and encircle them. Attacker chimps generally conduct process of hunting. During process of hunting, Driver, barrier and chaser chimpanzees are being a part rarely. Unfortunately, they are without any data regarding location of optimum (prey) within an abstract search space. To mathematically simulate chimp behaviour, this seems that best solution available (first attacker), driver, barrier and chaser had the information regarding potential prey location. Hence, acquired four of best solutions can be stored and existing chimps can be compelled for updating its positions based on locations of best chimps. This relationship can be discussed through Equation. (22) – (24).

$$d_{Attacker} = |c_1 x_{Attacker} - m_1 x|, d_{Barrier} = |c_2 x_{Barrier} - m_2 x|,$$
$$d_{Chaser} = |c_3 x_{chaser} - m_3 x|, d_{Driver} = |c_4 x_{Driver} - m_4 x|. \quad (22)$$

$$x_1 = x_{Attacker} - a_1(d_{Attacker}), x_2 = x_{Barrier} - a_2(d_{Barrier}),$$
$$x_3 = x_{Chaser} - a_3(d_{Chaser}), x_4 = x_{Driver} - a_4(d_{Driver}). \quad (23)$$

$$x(t+1) = \frac{x_1 + x_2 + x_3 + x_4}{4} \quad (24)$$

Here, the prey position can be evaluated through four best groups as well as remaining chimps randomly update its positions in vicinity.

Prey attacking (utilization)

As previously mentioned, during last stage, chimps will attack prey which complete hunt once after prey stops moving. f value should be decreased to mathematically model process of attacking. Note that **a** variation range can be decreased by **f**. Alternatively, **a** denotes random variable in interval [−2**f**, 2**f**], and f value decreases from 2.5 to 0 during iterations. Chimpanzee's next position can be anywhere between their current position and prey's position when random values of lie in range [−1, 1].

ChOA permits chimps for updating the positions based on the four types of chimps, Chimpanzee's positions which attack prey based on operators that have already been presented. ChOAs remains in danger for getting trapped in local minimum, whereas existing operators can be needed to prevent such problem. Proposed mechanism of driving, blocking, and chasing indicates process of exploration, ChOA needs additional operators for emphasising phase of exploration.

Searching for Prey (exploration)

As stated earlier, process of exploration between chimps can be primarily completed considering attacker, barrier, chaser, and driver Chimpanzee's location which can diverge in search for prey which aggregate for attacking prey. Mathematically model behaviour of divergence, **a** vector having random value larger than 1 or less than −1 can be utilized, search agents can be urged for diverging and getting distant from prey. The procedure indicates process of exploration which permits ChOA to find globally. In this method, the inequality |a|>1 drives chimps for getting scattered in habitat in search of better prey. GWO had influenced this section (Mirjalili, 2013).

Remaining component of ChOA influences phase of exploration to be c value. Elements of c vector could be random variables within interval [0, 2], as in equation (4). Such component gives random weights to prey enhance (c >1) or reduce (c<1) prey location effect on distance determination in equation (5). This assists ChOA improve their stochastic behaviour along process of optimization which decreases trapping chance in local minimum. **c** often requires to produce random values which execute process of exploration during initial iterations and final iterations. Especially during final iterations, the factor can be highly helpful to avoid local minimum. **c** vector can also consider as obstacles impact which secure chimps getting near to prey. Generally, natural impediments in the chimps' path secure from prey at good speed. It can be precise expression of effect of **c** vector. c vector assigns a random weight to prey based on position of chimp, for making hunt easier or harder.

Social incentive (sexual motivation)

Aforementioned, obtaining meet as well as following social motivation (sex as well as grooming) during last stage makes chimpanzees

relinquish the responsibilities of hunting. Hence, chimps attempt for obtaining meat forcefully chaotic. During final stage, such chaotic behaviour of chimps used to alleviate two entrapment problems in rate of slow convergence as well as local optimum to solve problems of high-dimensional.

Chaotic maps are utilized for enhancing performance of ChOA which are discussed. Six chaotic maps have been utilized. The maps are processes of deterministic with random behaviour. In this study, the number 0.7 was chosen to be major reference point for entire maps (Saremi, Mirjalili, & Lewis, 2014). Value 0.7 was taken to be maps' principal reference point, regarding Saremi, Mirjalili, & Lewis, 2014 in this research. There is 50% chance for selecting either normal updating model of chaotic or mechanism of position for updating chimps' position in optimization to represent such simultaneous behaviour. Mathematical model has been detailed through equation (25).

$$x_{chimp}(t+1) = \begin{cases} x_{prey}(t) - a.dif\mu < 0.5 \\ Chaotic\_value if\mu \geq 0.5 \end{cases} \quad (25)$$

Here μ denotes random number in [0, 1].

Briefly, ChOA search process begins with producing chimps' stochastic population (candidate solutions). Attacker, barrier, chaser, and driver are four predefined independent groups are can be randomly categorised entire chimps. Through group strategy, every chimp updates their **f** coefficients. The four types of chimps evaluate approximate locations of prey in iteration period. Every candidate's distance from the prey is updated. Avoidance of Local optimum and a curve of faster convergence are created simultaneously by **c** and **m** vectors' adaptive tuning. For enhancing exploitation process as well as prey attacking, **f** value is decreased from 2.5 to zero. Inequality | a | > 1 causes candidate solutions divergence, or else they will ultimately converge on the prey.

4.5 Proposed Oppositional based Chimp Optimization Algorithm

In proposed algorithm, concept of opposition based learning is embedded into standard ChOA for enhancing the ChOA performance as well as their convergence speed. The detailed implementation procedure of OChOA for optimal selection can be described as follows.

Opposition based initialization

To regulate size of opposition's step, a_i and b_i should dynamically update regarding current population's search space. This shows that every dimension's minimum and maximum values in current population can be utilized for calculating the opposite solution other than boundaries of predefined interval ([a_i, b_i]). Pigeons are aided in their search for better positions by dynamic opposition, which speeds up convergence. It is possible to compute a new opposition-based approach:

$$OP_{i,j} = a_j^p + b_j^p - P_{i,j} \quad (26)$$

Here $P_{i,j}$ denotes j-th position vector of i-th chimp within population, $OP_{i,j}$ denotes opposite position of $P_{i,j}$, $a^p{}_j$ as well as $b^p{}_j$ respectively denote j-th dimension's minimum and maximum values in current population. Fig.5 shows the flow chart of the proposed oppositional based chimp optimisation –LSTM model.

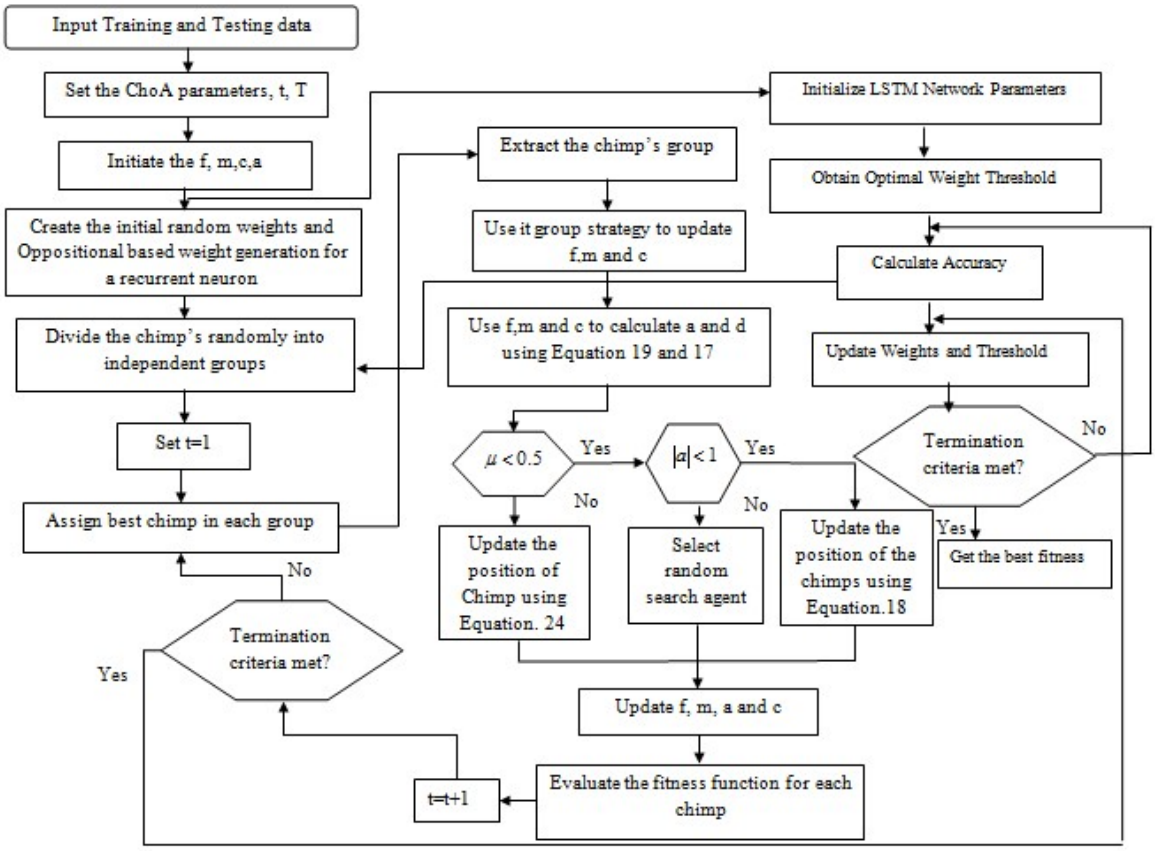

Fig.5 Flow chart of the proposed OChOA-(LSTM) RNN model

The training and testing phase is as shown in the Fig.6.

Fig.6 Training and Testing phase involved in OChOA-RNN

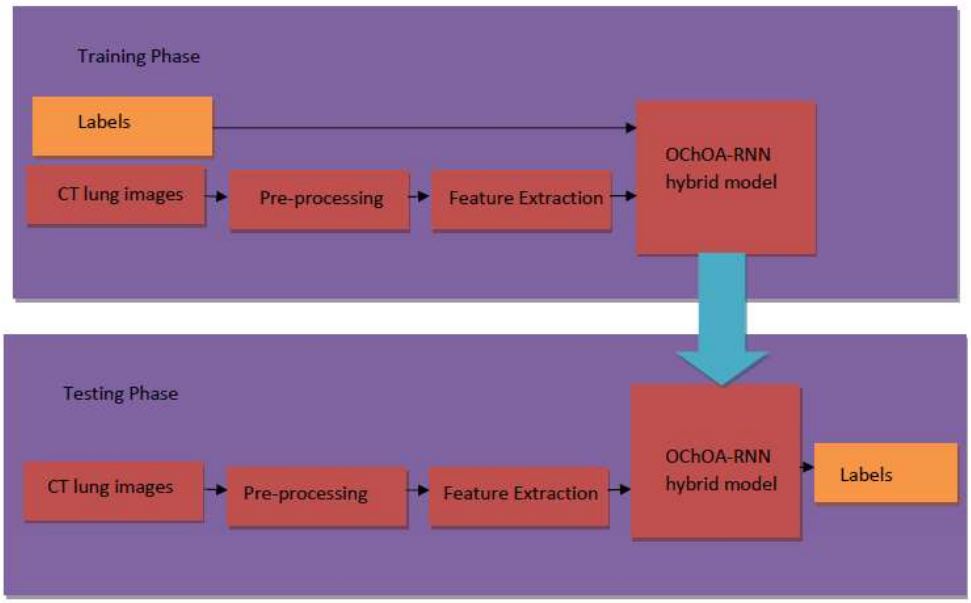

Table 3 shows the initial parameters used by CHOA,PSO,SSO and GA for optimising the weights and bias of LSTM network with Accuracy being the fitness function.

Table 3 Initial Parameters for optimization of LSTM network

Algorithms	Parameter	Value
ChOA	a	[1,1]
	f	linearly decreased from 2 to 0
	Maximum number of Iterations	1000
	Number of search agent	10
PSO	Number of Particle	10 and 50
	C1 :Importance of personal best value	C1+C2=4
	C2:Importance of Neighborhood best value	
SSO	Spider numbers	10
	Maximum number of iterations	1000
	Population size	10
GA	N: Population size, typically 10 to 40	n=10
	Lower bound limit and upper bound limit	lb= -10; ub = 10
	Maximum number of iterations	Max iter=1000

4. RESULTS AND DISCUSSION

The proposed OChOA-RNN, which was trained on Kaggle dataset participants with lung nodules performed exceptionally well to identify highly accuracy benign and malignant nodules in one-fifth of patients having nodules in small-to-intermediate size. It shows potential RNN value for risk prediction decision support of lung cancer in detected nodules of lung incidentally. Unnecessary workup such as procedures of imaging and invasive are neglected for large number of patients if CT scans are ruled out with high sensitivity (95.88 % in this study). Before deciding if it may be used in screening program of lung cancer, it has to be prospective validation. The research includes 120 benign images, 561 malignant images and 416 normal images for training and validating the model.

Traditional researches have analysed to maximize cancers proportion correctly characterized (that is, high positive-predictive value) which expressed authenticity. Even with most of the studies, such as big nodules up to 30 mm diameter, sensitivity of such tools remains moderate, limiting its clinical applicability, and not clinically relevant nodules in small-to-intermediate sized. Contrastingly utilizing AI for identifying lung cancers, the method evaluated for this study was utilized in system of AI called LCP-CNN, for identifying high degree of certainty in benign nodules which propose these nodules and are ruled out, securing requirement in upcoming process.

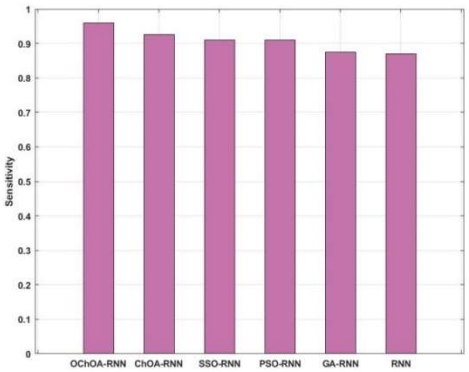

(a)

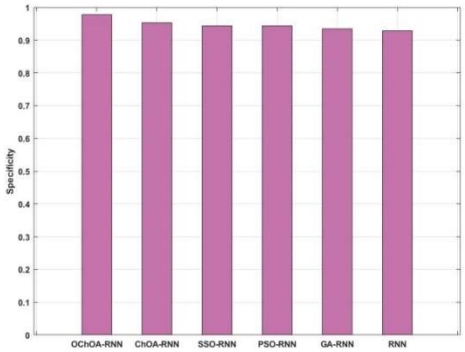

(b)

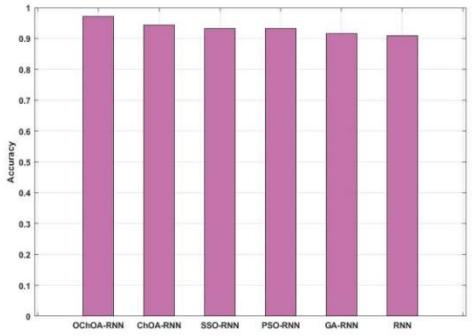

(c)

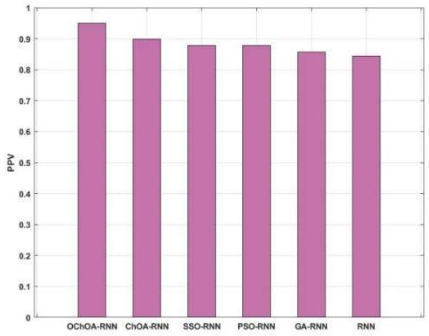

(d)

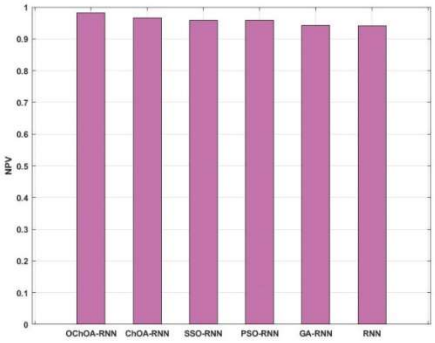

(e)

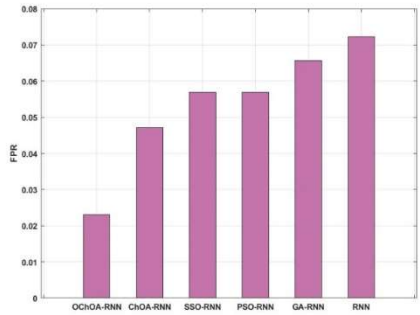

(f)

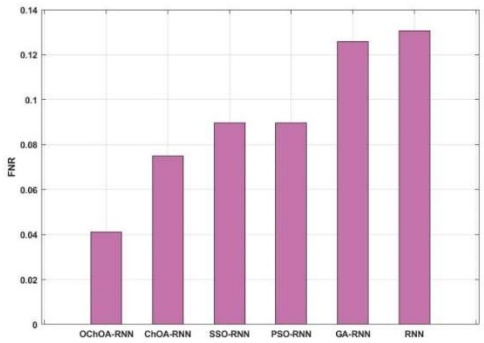

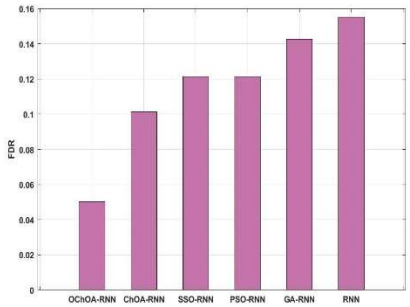

Figure: 7, performance measures with respect to different techniques

Table . 4 Performance analysis for Training Datasets

	Sensitivity	Specificity	Accuracy	PPV	NPV	FPR	FNR	FDR
Ochoa_RNN	**0.95232**	**0.992972**	**0.980507**	**0.983585**	**0.979207**	**0.007028**	**0.04768**	**0.016415**
ChOA_RNN	0.919898	0.988192	0.967251	0.971793	0.965394	0.011808	0.080102	0.028207
SSO_RNN	0.863954	0.970762	0.938012	0.928913	0.941642	0.029238	0.136046	0.071087
PSO_RNN	0.827718	0.940118	0.905653	0.859406	0.925035	0.059882	0.172282	0.140594
GA_RNN	0.811825	0.926061	0.891033	0.829221	0.917549	0.073939	0.188175	0.170779
RNN	0.800381	0.91594	0.880507	0.808087	0.912094	0.08406	0.199619	0.191913

Table . 5 Performance analysis for Testing Datasets

	Sensitivity	Specificity	Accuracy	PPV	NPV	FPR	FNR	FDR
OChoA-RNN	0.9588	0.9769	0.9713	0.9496	0.9812	0.0230	0.0411	0.0503
ChOA-RNN	0.92493	0.95290	0.94419	0.8988	0.9655	0.0470	0.0750	0.1011
SSO-RNN	0.91041	0.94304	0.93288	0.8785	0.9587	0.0569	0.0895	0.1214
PSO-RNN	0.91041	0.94304	0.93288	0.8785	0.9587	0.0569	0.0895	0.1214
GA-RNN	0.87409	0.93428	0.91553	0.8574	0.9425	0.0657	0.1259	0.1425
RNN	0.86924	0.92771	0.90950	0.8447	0.9400	0.0722	0.1307	0.1552

Figure 7 and table 4 and Table 5 shows the performance analysis of training and testing datasets over comparative techniques, it is evident from the investigation that incorporation of opposition strategy enhance the performance of traditional ChOA in predicting weights for RNN. The proposed model achieves accuracy of 97.13% that is 2.72% better than traditional ChOA associates RNN, 3.85% greater than SSO associates RNN and PSO associates RNN, 5.58% greater than GA associates RNN and 6.18% better than traditional RNN.

5. CONCLUSION

The purpose of identifying lung diseases successfully done through OChOA-RNN, the performance of proposed approach is superior over comparative techniques. Proposed technique attains an accuracy of 97.13% that is greater over comparative optimization associates RNN and far better than traditional RNN. It is evident from the investigative results that incorporation of opposition strategy enhances the performance by decreases the best solution gets escapes from a local optimum. In the future, this research intends to identify the appropriate weight value of RNN through other optimization techniques to enhance the performance further while diagnosing health care's diseases.

REFERENCES

[1]Sharma, Parvarish, Meenu Mehta, Daljeet Singh Dhanjal, Simran Kaur, Gaurav Gupta, Harjeet Singh, Lakshmi Thangavelu et al. "Emerging trends in the novel drug delivery approaches for the treatment of lung cancer." Chemico-biological interactions 309 (2019): 108720.

[2]Sadhasivam, Janani, and Abimanyu Sugumaran. "Magnetic nanocarriers: Emerging tool for the effective targeted treatment of lung cancer." Journal of Drug Delivery Science and Technology 55 (2020): 101493.

[3]Fujii, Kiyonaga, Haruhiko Nakamura, and Toshihide Nishimura. "Recent mass spectrometry-based proteomics for biomarker discovery in lung cancer, COPD, and asthma." Expert review of proteomics 14, no. 4 (2017): 373-386.

[4]World Cancer Report (2014) World Health Organization, Chapter 5.1. ISBN 92-832-0429-8

[5] https://www.naaccr.org/

[6]. Lung Cancer—Patient Version. NCI. Archived from the original on 9 March 2016. Retrieved 5 Mar 2016

[7]Cao, Maomao, and Wanqing Chen. "Epidemiology of lung cancer in China." Thoracic cancer 10, no. 1 (2019): 3-7.

[8]Yang, Dawei, Yang Liu, Chunxue Bai, Xiandong Wang, and Charles A. Powell. "Epidemiology of lung cancer and lung cancer screening programs in China and the United States." Cancer letters 468 (2020): 82-87.

[9] Wang, Dennis, Nhu-An Pham, Jiefei Tong, Shingo Sakashita, Ghassan Allo, Lucia Kim, Naoki Yanagawa et al. "Molecular heterogeneity of non-small cell lung carcinoma patient-derived xenografts closely reflect their primary tumors." International journal of cancer 140, no. 3 (2017): 662-673.

[10]Shanthi, S., and N. Rajkumar. "Lung cancer prediction using stochastic diffusion search (SDS) based feature selection and machine

learning methods." Neural Processing Letters 53, no. 4 (2021): 2617-2630.

[11]Liu, Xinglong, Fei Hou, Hong Qin, and Aimin Hao. "A CADe system for nodule detection in thoracic CT images based on artificial neural network." Science China Information Sciences 60, no. 7 (2017): 072106.

[12]Al Mohammad, Badera, Patrick C. Brennan, and Claudia Mello-Thoms. "A review of lung cancer screening and the role of computer-aided detection." Clinical radiology 72, no. 6 (2017): 433-442.

[13]Masood, Anum, Bin Sheng, Ping Li, Xuhong Hou, Xiaoer Wei, Jing Qin, and Dagan Feng. "Computer-assisted decision support system in pulmonary cancer detection and stage classification on CT images." Journal of biomedical informatics 79 (2018): 117-128.

[14]Khanmohammadi, Akbar, Ali Aghaie, Ensieh Vahedi, Ali Qazvini, Mostafa Ghanei, Abbas Afkhami, Ali Hajian, and Hasan Bagheri. "Electrochemical biosensors for the detection of lung cancer biomarkers: A review." Talanta 206 (2020): 120251.

[15] Bhandary, Abhir, G. Ananth Prabhu, V. Rajinikanth, K. Palani Thanaraj, Suresh Chandra Satapathy, David E. Robbins, Charles Shasky, Yu-Dong Zhang, João Manuel RS Tavares, and N. Sri Madhava Raja. "Deep-learning framework to detect lung abnormality–A study with chest X-Ray and lung CT scan images." Pattern Recognition Letters 129 (2020): 271-278.

[16] Toğaçar, Mesut, Burhan Ergen, and Zafer Cömert. "Detection of lung cancer on chest CT images using minimum redundancy maximum relevance feature selection method with convolutional neural networks." Biocybernetics and Biomedical Engineering 40, no. 1 (2020): 23-39.

[17] Gong, Jing, Ji-yu Liu, Yao-jun Jiang, Xi-wen Sun, Bin Zheng, and Sheng-dong Nie. "Fusion of quantitative imaging features and serum biomarkers to improve performance of computer-aided diagnosis scheme for lung cancer: A preliminary study." Medical physics 45, no. 12 (2018): 5472-5481.

[18] Masood, Anum, Po Yang, Bin Sheng, Huating Li, Ping Li, Jing Qin, Vitaveska Lanfranchi, Jinman Kim, and David Dagan Feng. "Cloud-based automated clinical decision support system for detection and diagnosis of lung cancer in chest CT." IEEE journal of translational engineering in health and medicine 8 (2019): 1-13.

[19] Gao, Ni, Sijia Tian, Xia Li, Jian Huang, Jingjing Wang, Sipeng Chen, Yuan Ma, Xiangtong Liu, and Xiuhua Guo. "Three-dimensional texture feature analysis of pulmonary nodules in CT images: lung cancer predictive models based on support vector machine classifier." Journal of digital imaging 33, no. 2 (2020): 414-422.

[20] Meldo, Anna, Lev Utkin, Maxim Kovalev, and Ernest Kasimov. "The natural language explanation algorithms for the lung cancer computer-aided diagnosis system." Artificial Intelligence in Medicine 108 (2020): 101952.

[21]Woźniak, Marcin, Dawid Połap, Giacomo Capizzi, Grazia Lo Sciuto, Leon Kośmider, and Katarzyna Frankiewicz. "Small lung nodules detection based on local variance analysis and probabilistic neural network." Computer methods and programs in biomedicine 161 (2018): 173-180.

[22] Shakeel, P. Mohamed, M. A. Burhanuddin, and Mohammad Ishak Desa. "Automatic lung cancer detection from CT image using improved deep neural network and ensemble classifier." Neural Computing and Applications (2020): 1-14.

[23] Singh, Gur Amrit Pal, and P. K. Gupta. "Performance analysis of various machine learning-based approaches for detection and classification of lung cancer in humans." Neural Computing and Applications 31, no. 10 (2019): 6863-6877.

[24]ALzubi, Jafar A., Balasubramaniyan Bharathikannan, Sudeep Tanwar, Ramachandran Manikandan, Ashish Khanna, and Chandrasekar Thaventhiran. "Boosted neural network ensemble classification for lung cancer disease diagnosis." Applied Soft Computing 80 (2019): 579-591.

[25] Shakeel, P. Mohamed, Amr Tolba, Zafer Al-Makhadmeh, and Mustafa Musa Jaber. "Automatic detection of lung cancer from biomedical data set using discrete AdaBoost optimized ensemble learning generalized neural networks." Neural Computing and Applications 32, no. 3 (2020): 777-790.

[26]Shakeel, P. Mohamed, Mohd Aboobaider Burhanuddin, and Mohamad Ishak Desa. "Lung cancer detection from CT image using improved profuse clustering and deep learning instantaneously trained neural networks." Measurement 145 (2019): 702-712.

[27] Varadharajan, R., M. K. Priyan, Parthasarathy Panchatcharam, S. Vivekanandan, and M. Gunasekaran. "A new approach for prediction of lung carcinoma using back propogation neural network with decision tree classifiers." Journal of Ambient Intelligence and Humanized Computing (2018): 1-12.

[28]Lakshmanaprabu, S. K., Sachi Nandan Mohanty, K. Shankar, N. Arunkumar, and Gustavo Ramirez. "Optimal deep learning model for classification of lung cancer on CT images." Future Generation Computer Systems 92 (2019): 374-382.

[29]Schwyzer, Moritz, Daniela A. Ferraro, Urs J. Muehlematter, Alessandra Curioni-Fontecedro, Martin W. Huellner, Gustav K. Von Schulthess, Philipp A. Kaufmann, Irene A. Burger, and Michael Messerli. "Automated detection of lung cancer at ultralow dose PET/CT by deep neural networks–initial results." Lung Cancer 126 (2018): 170-173.

[30] R.M. Haralick, Statistical and structural approaches to texture, in: Proceedings of the IEEE, vol. 67, 1979, pp. 786–804.

[31] R.M. Harlick, K. Shanmugam, I. Dinstein, IEEE trans, Sys. Man Cybern. 3 (1973) 610–621.

[32] D.G. Barber, E.F. LeDrew, SAR sea ice discrimination using texture statistics: a multivariate approach, Photogrammetric Engineering and Remote Sensing 57 (4 (April)) (1991) 385–395.

[33] J.L. Raheja, K. Das, A. Chaudhary, Fingertip detection: a fast method with natural hand, IJESC 3 (2 December) (2011) 85–89.

[34] Liu, Liyuan, Meng Han, Yiyun Zhou, and Yan Wang. "Lstm recurrent neural networks for influenza trends prediction." In International Symposium on Bioinformatics Research and Applications, pp. 259-264. Springer, Cham, 2018.

[35] Su, Peng, Xiao-Rong Ding, Yuan-Ting Zhang, Jing Liu, Fen Miao, and Ni Zhao. "Long-term blood pressure prediction with deep recurrent neural networks." In 2018 IEEE EMBS International conference on biomedical & health informatics (BHI), pp. 323-328. IEEE, 2018.

[36] Nowak, Jakub, Ahmet Taspinar, and Rafał Scherer. "LSTM recurrent neural networks for short text and sentiment classification." In International Conference on Artificial Intelligence and Soft Computing, pp. 553-562. Springer, Cham, 2017.

[37]Wielgosz, Maciej, Andrzej Skoczeń, and Matej Mertik. "Using LSTM recurrent neural networks for monitoring the LHC superconducting magnets." Nuclear Instruments and Methods in Physics Research Section A: Accelerators, Spectrometers, Detectors and Associated Equipment 867 (2017): 40-50.